Journal of Molecular Catalysis A: Chemical 344 (2011) 111–121

Contents lists available at ScienceDirect

Journal of Molecular Catalysis A: Chemical

journal homepage: www.elsevier.com/locate/molcata

In situ FTIR studies of CO oxidation over Fe-free and Fe-promoted PtY catalysts: Effect of water vapor addition

Zeinhom M. El-Bahy[a,*], Ahmed I. Hanafy[a], Mohamed M. Ibrahim[a], Masakazu Anpo[b]

[a] Chemistry Department, Faculty of Science, Taif University, Taif, Saudi Arabia
[b] Department of Applied Chemistry, Graduate School of Engineering, Osaka Prefecture University, 1-1 Gakuen-cho, Naka-ku, Sakai, Osaka 599-8531, Japan

ARTICLE INFO

Article history:
Received 17 January 2011
Received in revised form 4 May 2011
Accepted 15 May 2011
Available online 23 May 2011

Keywords:
CO oxidation
CO adsorption
WGSR
In situ FTIR
CO-TPD
TEM

ABSTRACT

In the quest of better CO elimination catalysts, Fe oxide was employed to promote platinum supported on HY zeolite. Fe-free and Fe-promoted PtY catalysts were prepared by ion exchange method and calcined at 500 °C. The prepared samples were characterized using XRD, FTIR, TEM, CO adsorption and CO-TPD. The particles size calculated from XRD patterns and TEM images was ≈18–20 nm in PtY and ≈8–15 nm in PtFeY. The CO removal performance over the prepared solids has been investigated by means of in situ technique using FTIR spectroscopy. Platinum surface modified with Fe oxide has a pronounced catalytic activity towards the CO oxidation more than Fe-free Pt containing catalyst. Reduction of the prepared catalysts with H_2 gas prior to admission of gas mixtures increased the catalytic activity more than that of as prepared catalysts. A strong positive water-effect was established when a trace amount of water (more realistic conditions) was added to the gas mixture ($CO + O_2$) during the CO oxidation particularly over PtFeY. In presence of water, the amount of CO_2 adsorbed over PtFeY is ≈5 and ≈600 times more than that of water free reaction over PtFeY and PtY catalysts, respectively.

1. Introduction

Seeking for new energy resources never ends. Proton exchange membrane fuel cell (PEMFC) has been studied extensively in recent years and presented considerable promise for both stationary and automotive power supply using hydrogen fuel. Reforming of hydrocarbon fuels can provide a H_2-rich stream having an approximate composition of 45–75% H_2, 15–25% CO_2, 0.5–2% CO, 10–20% H_2O and N_2 [1]. CO causes a severe problem for platinum anode since it is seriously adsorbed on Pt sites and works as poisonous agent. Hence, the PEMFC efficiency decreases. The CO level in H_2 stream is needed to be less than 10 ppm [2]. CO traces may be removed by oxidation of CO with oxygen gas or with water in water gas shift reaction (WGSR).

Precious metals work very well with high catalytic activity and stability on CO oxidation at low temperature [3–5]. A large number of catalysts have been studied for the CO oxidation; however, the quest for catalysts of higher catalytic activity at lower temperatures is never-ending. The catalytic behavior of supported Pt has been found to be unique among the noble metals in CO oxidation. Supported Pt [6–8] catalyzes selective CO oxidation but the selectivity to form CO_2 is below 60%, even at low reaction temperatures (<220 °C).

The adsorption and catalytic properties of Pt are not only influenced by a complex set of contributions of the particle morphology, metal dispersion and electronic properties of the metal, but also are affected by the presence of other metal ions that act as dopants for Pt atoms. Arnby et al. reported that modifying Pt–Al_2O_3 system by Fe-oxide increased the tolerance towards hexamethyldisiloxane (HMDS) [9]. The activity and selectivity of CO oxidation in PROX reaction increased significantly after promotion of Pt/mordenite with Fe [10]. In these oxide promoted catalysts, the activity is likely to be controlled via the Pt-promoter interface and so it is imperative that the oxide and Pt should be associated together to maximize the catalytic activity [11,12]. This can be difficult to be ensured using conventional preparation methods such as impregnation or co-precipitation. One of the ways to avoid this is to use ion exchange method to homogenously distribute ions all over the surface.

Although aluminum is the most common support for noble metal-based catalysts, recent studies have indicated that the use of zeolites as supports for Pt catalysts is promising to improve the catalytic activity and selectivity [13]. In particular, PtY catalyst resulted in a good catalytic activity as membrane in PROX [14] and in CO oxidation reaction in aqueous phase [15]. Accordingly, it is needed to elucidate the effect of supporting bimetallic system (Pt and Fe) on the high surface area and high acidity HY zeolite. It is well known that, the active sites are closely related with the type of support, promoter and the oxidation state of the Pt species on the surface, so that reduction of Pt species is crucial to understand the type of CO-surface interaction and CO removal mechanism.

* Corresponding author.
E-mail address: zeinelbahy2020@yahoo.com (Z.M. El-Bahy).

1381-1169/$ – see front matter © 2011 Elsevier B.V. All rights reserved.
doi:10.1016/j.molcata.2011.05.008

Water vapor showed inhibiting effect on the catalytic activity in some reactions such as the combustion of styrene over copper based catalysts [16], CO oxidation over Au/TiO_2–In_2O_3 catalyst [17], selective catalytic reduction of NO over Pd-ZSM-5 [18] and CO oxidation over Pt–Au/CeO_2 [19]. On the other hand, water showed great enhancing effect on the catalytic activity of several reactions such as CO oxidation over a commercial three-way catalysts [20], Pt–Pd/CeO_2 catalysts [21], Pt-NaY and Au-NaY in aqueous solution [15] and Pt/Al_2O_3 [22]. Addition of water increased the catalytic activity and decreased the oxidation temperature. Due to the effect of adsorption completion of water and CO or oxygen, it will be important to use small amount of water to minimize the competitive adsorption of water and reactants in the reaction medium.

The aim of this study is to investigate the effect of Fe-promotion on the catalytic activity of PtY catalyst in CO elimination via oxidation by O_2 gas or by water in WGSR using in situ FTIR technique. Moreover, the influence of addition of trace amount of water on the oxidation of CO by O_2 gas is one of the important targets of this study.

2. Experimental

2.1. Catalyst preparation

2.1.1. Preparation of PtY

PtY catalyst was prepared by conventional ion exchange method, briefly, a sample (4 gm) of HY (Toyota Company Ltd., Japan) was added to 0.01 M solution of $Pt(NH_3)_4Cl_2{\cdot}H_2O$ (Mtsuwa's Pure Chemicals) and the slurry (pH = 6.2) was stirred for 24 h at room temperature. The suspension was filtered off, and the process was repeated three times until almost complete exchange was obtained. The Pt content was measured by atomic absorption spectroscopy using Varian atomic absorption spectrometer (Shimadzu AA-6400F) and it was found to be ≈1.2 wt.%. The prepared sample will be referred as PtY.

2.1.2. Preparation of bimetallic PtFeY

PtFeY was prepared by successive ion exchange method of Fe^{3+} and Pt^{2+} to HY zeolite. 4 gm of HY zeolite was stirred with 0.01 M $FeCl_3{\cdot}9H_2O$ for 1 h at room temperature. The solution was centrifuged, washed with distilled water, dried at 100 °C for 24 h and finally calcined at 500 °C for 3 h. Platinum was added to the FeY powder as a solution of $Pt(NH_3)_4Cl_2{\cdot}H_2O$ (0.01 M) at pH = 10 (NaOH was used to adjust pH value). Pt solution was stirred with FeY at 80 °C for 1 h. The solution was then filtered, washed with distilled water and finally dried at 100 °C for 24 h. The platinum concentration in the sample was almost the same like PtY sample. The Fe-promoted PtY sample will be referred as PtFeY.

Reduction of the catalysts was performed in static conditions in presence of 80 Torr of pure hydrogen atmosphere at 400 °C for 30 min in presence of liquid nitrogen trap to collect the produced H_2O to not re-oxidize the surface species once again. Reduced samples will be referred as Pt*Y and Pt*FeY for unpromoted and Fe-promoted catalysts, respectively.

2.2. Catalyst characterization

X-ray powder diffraction (XRD) patterns of the prepared solids were recorded at room temperature using a model Bruker axs, D8Advance. Average crystallite size (D) of the obtained powders were calculated by X-ray line broadening technique performed on the direction of lattice using the so-called Hall-equation–Scherrer's formula $D = 0.89\lambda/\beta \cos\theta$ [23], where D is the crystallite size, λ represents the X-ray wavelength (1.5404 Å), β is the full width at half the maximum intensity (FWHM) in radians, and θ is the Bragg's angle.

IR spectra were recorded in the solid mixture of sample and KBr as pellets on JASCO FTIR-600 Plus with a spectral resolution of 2 cm^{-1} and accumulation of 100 scans at room temperature.

Temperature programmed desorption (TPD) experiments were carried out using CO as a probe molecule to determine the basicity properties of the prepared solids. TPD experiment was performed in a fixed-bed reactor system. Prior to TPD measurements, the catalyst (30 mg) was treated at its activation temperature 500 °C for 1 h in air and then evacuated for 1 h at the same temperature and 10^{-4} Torr. The sample was then cooled under the same pressure until room temperature. After cooling, 7 Torr of CO gas were adsorbed on the surface of the sample and equilibrated for 30 min. The CO molecules in gas phase were degassed at room temperature for 1 h. The degassed CO molecule ($m/z = 28$) was monitored by a gas desorption analyzer (Anelva, M-QA100TS) equipped with a quadruple mass analyzer in a high-vacuum chamber of 7.5×10^{-9} Torr range. TPD profiles were recorded by linear heating of the samples from 25 to 500 °C at constant ramp rate of 5°/min. To compare the possibility of CO_2 desorption out of the surface, $CO + O_2$ (7:7) gas mixture was admitted to the employed catalysts. The catalyst sample was saturated with the gas mixture at room temperature for 30 min after which the sample was degassed at room temperature for 1 h. The experiment was then completed as mentioned above except that the CO_2 molecule ($m/z = 44$) in the temperature range of 25–700 °C was detected.

Transmission electron microscope (TEM) micrographs were measured using JEOL JEM-1010 transmission electron microscope at an accelerating voltage of 60 kV. Suspensions of the samples were put on carbon foil with a micro grid. TEM images were observed with minimum electron irradiation to prevent damage to the sample structure.

The FTIR spectra were recorded on JASCO FTIR-660 Plus with a spectral resolution of 2 cm^{-1} and accumulation of 32 scans. Briefly, self-supporting pellets (ca. 15–20 mg cm^{-2}) were prepared from the sample powder and treated directly in the purpose-made IR quartz cell equipped with $CaCl_2$ windows. The latter was connected to a vacuum-adsorption system with a residual pressure below 10^{-4} Torr. Before the adsorption measurements, the samples were heated at 500 °C for 2 h in air followed by 1 h evacuation at same temperature. After pretreatment, the catalysts were cooled at room temperature (RT) before admission of CO gas (10 Torr). After CO admission, the cell was left to equilibrate for 30 min after which the sample was evacuated for 20 min at room temperature. The FTIR cell was sealed with built in stopcock removed from the vacuum line and then was placed in the FTIR instrument for spectra measurements. Background spectrum was subtracted from the collected spectra at each step to evaluate the spectral changes due to CO admission.

2.3. Catalytic activity measurements

Monitoring the events taking place in catalytic materials under reaction conditions is essential for understanding the reaction mechanism of many important chemical processes and would help to the rational design of new or better catalysts. The reaction can be monitored by in situ FTIR technique. As a typical reaction experiment, the samples were activated by keeping for 2 h at 500 °C in air followed by 1 h evacuation at same temperature. The cell was allowed to cool to RT prior to admitting reaction gases. The same procedure mentioned in CO adsorption section was followed in the gas mixture reaction. The selectivity and CO conversion depend mainly on the O_2/CO ratio. Previous reports stated that the highest catalytic activity and selectivity were obtained when O_2/CO ratio equals one [21,24]. Thus, the ratio O_2/CO = 1 was chosen to be used in the present study. In situ FTIR spectra of PtY and PtFeY catalysts were obtained under reaction gas mixture conditions of

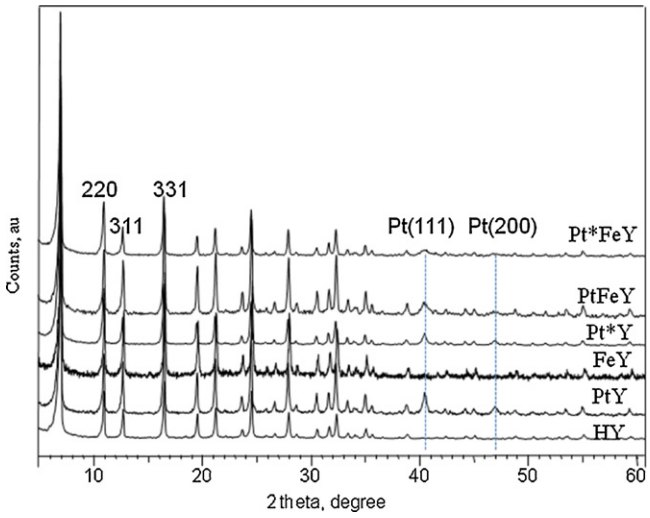

Fig. 1. X-ray powder diffraction patterns of parent HY, PtY and Fe-promoted PtY catalysts.

$CO:O_2 = 10:10$ (20), $CO:H_2O = 15:1$ (16) and $CO:O_2:H_2O = 15:15:1$ (31) where the values in parenthesis denotes to the total pressure in the cell. The reaction was carried out at different temperatures ranging from RT to 100 °C and the spectra are shown in the wavenumber range of 2400–1500 cm^{-1}.

3. Results and discussions

3.1. Characterization of the prepared catalysts

3.1.1. X-ray diffraction

The XRD patterns of parent HY and the prepared samples are shown in Fig. 1. The patterns exhibited the typical lines of parent HY zeolite indicating that the structure of the zeolite remains intact after inclusion of metal ions by ion exchange of Pt and/or Fe metal ions. With careful inspection of the XRD patterns, it can be observed that the exchanged cations, Pt or Fe, are randomly distributed within the lattice because $I_{331} > I_{220} > I_{311}$ [25]. Small lines were observed at 2θ values of 40.4° and 47° due to Pt(1 1 1) and Pt (2 0 0) particles, respectively [PDF# 87-0647]. The Pt particle size on the prepared solids was calculated using Scherrer's equation and it was found to be ≈19 nm and ≈12 nm for PtY and PtFeY, respectively, and these data are listed in Table 1. It was reported in literature that the particle size of Pt in Pt containing catalysts increased after promotion with Fe using incipient impregnation [8,12] or selective vapor deposition [2] preparation methods. In this study, the Pt particle size decreased due to the occlusion of Fe with Pt using ion exchange method. This is in accordance with earlier reports where Pt particles underwent more dispersion and less particle size after incorporation of ceria to alumina support [26]. The decrease of Pt particle size with the promotion of Fe indicates the effectiveness of such preparation method to form well homogeneously dispersed Pt particles over the support surface.

Table 1
Average particle size calculated from line broadening and TEM images.

Position	PtY	Pt*Y	PtFeY	Pt*FeY
Pt(1 1 1)	20.9	19.9	14.4	12.1
Pt(2 0 0)	18.8	18.6	16.2	18.1
TEM	≈20	≈18	≈15	≈8

3.1.2. FTIR spectroscopy

The framework IR spectra (not shown) of the prepared catalysts besides parent HY zeolite in the range of 1700–400 cm^{-1} exhibited bands of varying intensity and width at about 1184, 1054, 817, 746, 591 and 468 cm^{-1} which are typical for Y zeolite [27]. The structural insensitive vibrations caused by internal vibrations of $(Si,Al)O_4$ tetrahedra of HY were observed at 1054, 746 and 468 cm^{-1}, whereas the bands related to external linkages between $(Si,Al)O_4$ tetrahedra and are sensitive to the framework structure were observed at 1184, 817, and 591 cm^{-1} [28]. The absorption frequency of H_2O vapor was located at 1637 cm^{-1} [1,29]. Any peaks characteristic to either Pt–O or Fe–O bonds have not been observed which may be due to the low concentration of these oxides on the solid surface. The IR data confirmed that neither the structure-insensitive nor sensitive bands show any significant changes in the measured spectra as compared with the spectra of the host HY zeolite. These observations denote to the constancy of the zeolite framework during the preparation process which is the same observation concluded from XRD data.

3.1.3. Transmission electron microscope (TEM)

Fig. 2 shows the TEM images of the two dimensional distribution of PtY, Pt*Y, PtFeY and Pt*FeY catalysts onto the supporting carbon film. The TEM images of PtY and Pt*Y (Fig. 2a and b) show that the Pt particles are highly dispersed and have an average particle size in the range of 15–30 nm as shown in Table 1. The presence of Fe oxide in the promoted catalysts has an effect on the size of Pt metal particles as shown in Fig. 2c and d, where the particle size of the Fe promoted catalysts was in the range of 8–15 nm. The particle size values calculated from TEM images are very similar to that calculated from XRD patterns using the line broadening method.

3.1.4. Temperature programmed desorption (TPD)

The profiles of the desorbed CO *vs.* temperature for the prepared solids in the temperature range of 25–500 °C are shown in Fig. 3. CO-TPD profile of PtY catalyst shows only one wide peak due to CO desorption at 362 °C whereas the CO-TPD profile of FeY shows the CO desorption peak at 328 °C. In case of PtFeY desorption profile, two peaks can be observed, one at low temperature centered at 77 °C and the other at high temperature centered at 266 °C. The desorption values of PtY (at 362 °C) and FeY (at 328 °C) are anomalously high comparing to the desorption values of PtFeY sample (at 73 and 266 °C), i.e. PtY and FeY have higher molecular CO desorption energy due to the presence of high basicity sites. In case of Fe-free PtY catalyst, the Pt lattice is expanded parallel to the surface, the *d* states have to move up in energy which gives stronger interaction with CO and hence needs higher temperature to be desorbed out of surface [30]. The CO-TPD profiles show wide desorption peaks as a result of different activation energies for desorption, which means some heterogeneity in the adsorption sites on the surface [31,32]. These results indicated that the promotion with Fe caused electron-deficiency of the platinum in PtFeY. Moreover, it weakens the electron back-donation from platinum substrate to the adsorbed CO and weakens the CO–Pt bond, which induces the CO desorption at lower temperature [33,34]. The same observation was noticed in case of promoting Pt/Al_2O_3 with Mg ions in a previous work [35].

Fig. 4 shows the TPD profiles of CO_2 desorbed from PtY and PtFeY samples where CO was admitted together with O_2 ($CO + O_2$; 7:7). The temperature range of CO_2 desorption was divided into three regions as follows: low basicity sites where CO_2 was desorbed below 150 °C; medium basicity sites where CO_2 was desorbed below 400 °C; high basicity sites where CO_2 was desorbed over 400 °C. PtY catalyst exhibited a broad desorption peak around 450 °C, which assigned the presence of strong basic sites. For PtFeY catalyst, two CO_2 desorption peaks around 141 and 380 °C were

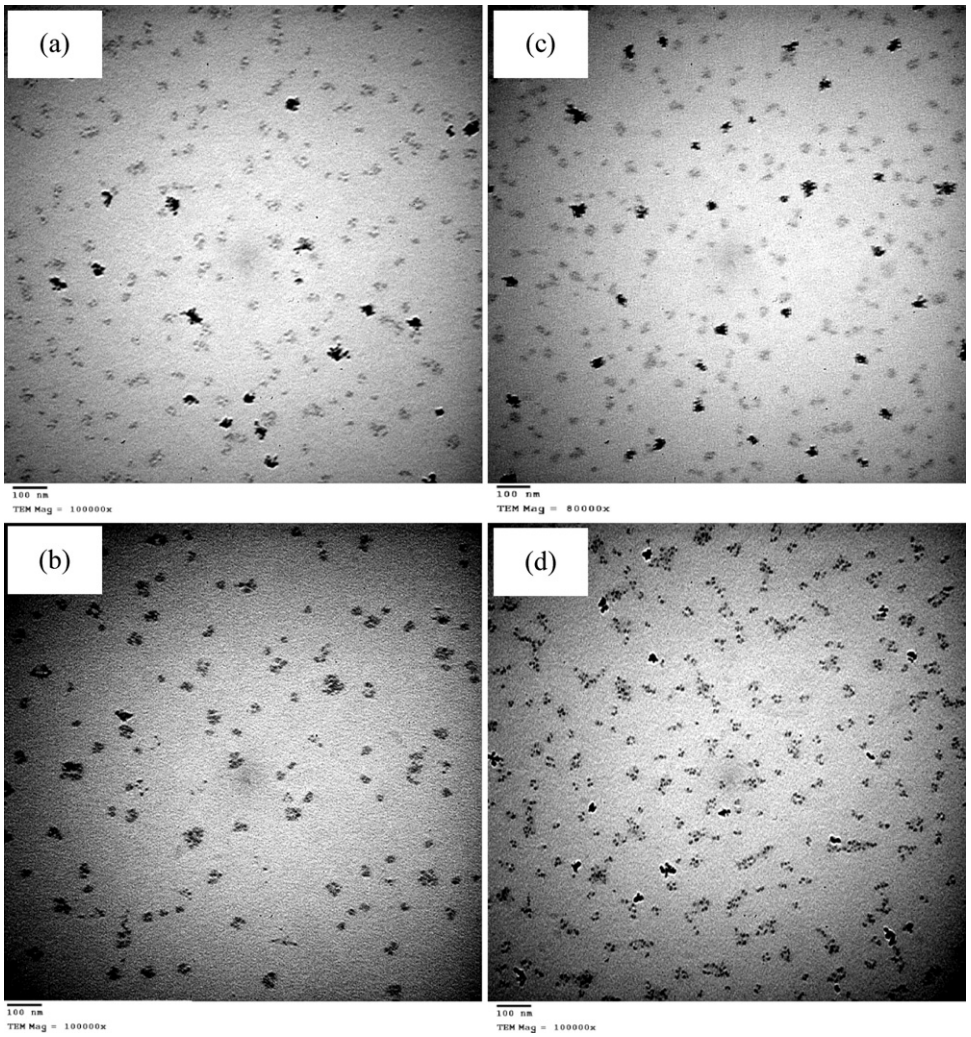

Fig. 2. The TEM images of as prepared PtY (A), Pt*Y (B), PtFeY (C), and Pt*FeY (D).

noticed. These peaks were assigned to weak and medium basic sites, respectively [35]. These data indicated that the possibility of CO_2 formation and desorption on PtFeY occur at lower temperature than on the surface of PtY. It is noteworthy to mention that, the TPD profiles of $m/z = 45$ and 46 (not shown) presented very low amounts of $m/z = 45$, due to formate species, and $m/z = 46$, due to formic acid. The profiles have the same shape of CO_2 for both PtY and PtFeY catalysts.

3.1.5. CO adsorption at room temperature

To determine the type and strength of CO adsorption species on PtY and Fe-promoted PtY catalysts, CO was admitted with a pressure of 10 Torr at room temperature to the as-prepared and reduced catalysts.

3.1.5.1. Adsorption of CO on PtY. The IR spectrum of CO adsorption on an activated PtY at RT (Fig. 5a) presents a group of small

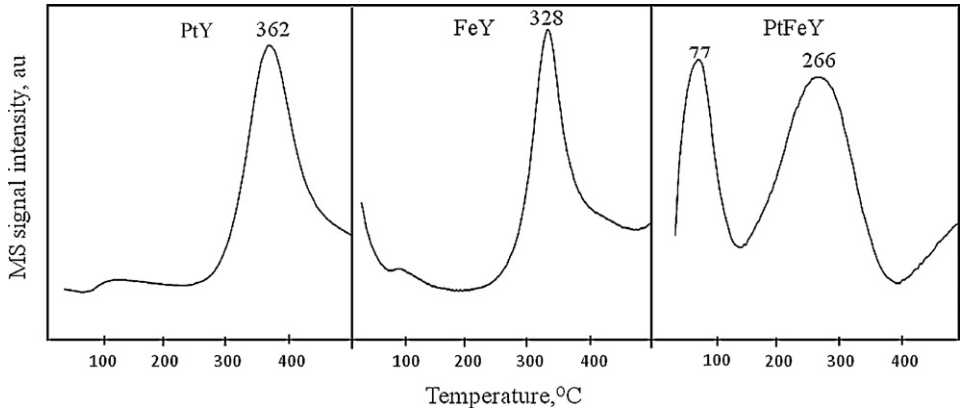

Fig. 3. CO-TPD profiles of PtY, FeY and PtFeY samples.

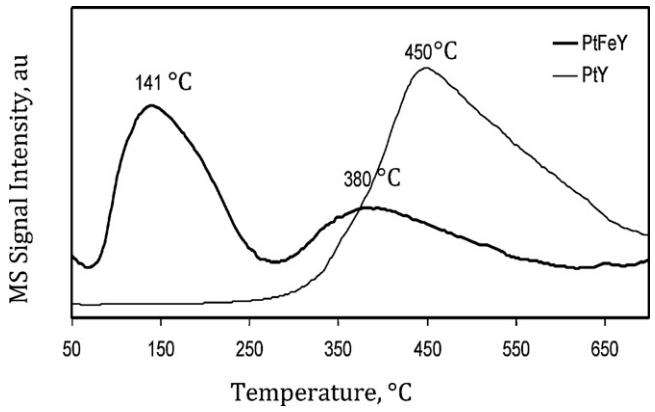

Fig. 4. TPD spectra of CO_2 desorption after $CO + O_2$ (7:7) adsorption over PtY and PtFeY catalysts.

peaks characteristic to CO adsorbed on different species of Pt^{n+} ($2 \geq n \geq 0$) at 2168, 2128, 2081 and small peak at 1885 cm^{-1}. In addition a peak at 1710 cm^{-1} due to CO oxidation products was also observed. According to literature data [36–38], the small peak at 2081 cm^{-1} is assigned to singleton frequencies of CO molecules linearly adsorbed on-top metallic Pt atoms (Pt^0–CO). The band at 2168 is assigned to CO adsorbed on oxidized platinum sites that are not in cationic positions [39] and the band at 2128 cm^{-1} is due to ν_s mode of carbonyl complexes formed with the participation of platinum cation $Pt^+(CO)_2$ [39–41]. The ν_{as} mode should be detected around ≈2091 cm^{-1}, so it may overlap with the peak at 2081 cm^{-1}. The small band at 1885 cm^{-1} is characteristic to CO adsorbed on two surface Pt atoms ($Pt^0{}_2CO$) [42]. The presence of Pt^0–CO and $Pt^0{}_2CO$ indicates that a fraction of Pt^{2+} was reduced by the freed free ammonia ligands, in precursor $[Pt(NH_3)_4]^{2+}$, during the activation process [43]. The band at 1710 cm^{-1} is due to carboxylate species (–COO^-) [44,45] which is an oxidation product of CO. After evacuation at RT, Fig. 5b, the peaks due to oxidized platinum sites decreased and the peak due to bridged $Pt^0{}_2CO$ diminished. The peak characteristic to carboxylate species abruptly increased after evacuation with the appearance of small peak due to adsorbed species of CO_2 at 2355 cm^{-1} [11,46].

The IR spectrum of CO adsorbed on Pt*Y at RT is shown in Fig. 5c. The spectrum showed one main peak at 2086 cm^{-1} and smaller peak at 1862 cm^{-1} which are due to linear Pt^0–CO and bridged $Pt^0{}_2CO$, respectively. Small intensity peak at 2172 cm^{-1} was observed as well indicating the presence of platinum oxidized species (Pt^{n+}) even after reduction with H_2. Carboxylate species was formed as CO oxidation products and detected at 1710 cm^{-1}. After evacuation at RT, Fig. 5d, the peaks at 1862 and 2172 cm^{-1} disappeared. Linear Pt^0–CO band underwent a red shift to 2075 cm^{-1} with an increase of the band characteristic to carboxylate species.

In absence of oxygen, CO may be oxidized by either oxygen attached with Pt cations or oxygen in zeolite framework. The decrease in the bands characteristic to CO adsorbed on Pt cationic species after admission of CO and the low intensity of the peak characteristic to carboxylate species formed over Pt*Y may point to the participation of the oxygen attached to Pt cations on the surface for CO oxidation.

3.1.5.2. Adsorption of CO on PtFeY. Fig. 6 shows the infrared spectra of CO adsorbed on PtFeY and Pt*FeY catalysts. The spectrum taken after CO adsorption over PtFeY at RT (Fig. 6a) displayed a well resolved absorption band at 2077 cm^{-1}, corresponding to linear Pt^0–CO with 4 cm^{-1} lower wavenumber than that of PtY sample (2081 cm^{-1}). In addition, small peaks at 2166 and 2125 cm^{-1} due to CO adsorbed on cationic Pt were observed. Another small peak at 1645 cm^{-1} was also detected which is due to carbonate species ($CO_3{}^{2-}$) [46].

Unfortunately, the corresponding Fe–CO peak (supposed to be at 2032 cm^{-1}) [47] couldn't be detected. If it happens, there will be superposition with linear Pt^0–CO, but most probably it does not happen at RT. Thus, the adsorption of CO occurs preferentially over Pt^{n+} sites rather than Fe^{3+} sites in the present experimental conditions. Consequently, all the peaks in the spectra are due to the adsorption of CO on Pt^{n+} ($2 \geq n \geq 0$) species as detected before in previous literature [11].

After evacuation at RT (Fig. 6b) the intensity of the peak characteristic to carbonate species increased with growing up a new peak at 1850 cm^{-1} due to bridged $Pt^0{}_2CO$. With increasing evacuation temperature to 50 °C (Fig. 6c) a red shift of the peak characteristic of Pt^0–CO from 2077 to 2068 cm^{-1} was observed with decreasing in its intensity. Also, a decrease in the peaks due to CO adsorbed on Pt^{n+} was observed accompanied by the disappearance of the peak due to bridged $Pt^0{}_2CO$.

The spectrum recorded after admission of 10 Torr of CO gas on the surface of Pt*FeY at RT (Fig. 6d) showed a peak characteristic to linear Pt^0–CO at 2077 cm^{-1} with 9 cm^{-1} lower wavenumber and higher intensity than that of Pt*Y sample (2086 cm^{-1}). Small amounts of CO adsorbed on cationic platinum and bridged $Pt^0{}_2CO$ species were observed at 2170 cm^{-1} and 1850 cm^{-1}, respectively. Carbonate species were also detected at 1641 cm^{-1} as well. With evacuation at RT and 50 °C (Fig. 6e and f) a red shift to the peak at 2077–2061 cm^{-1} was observed and a slight increase of the peak

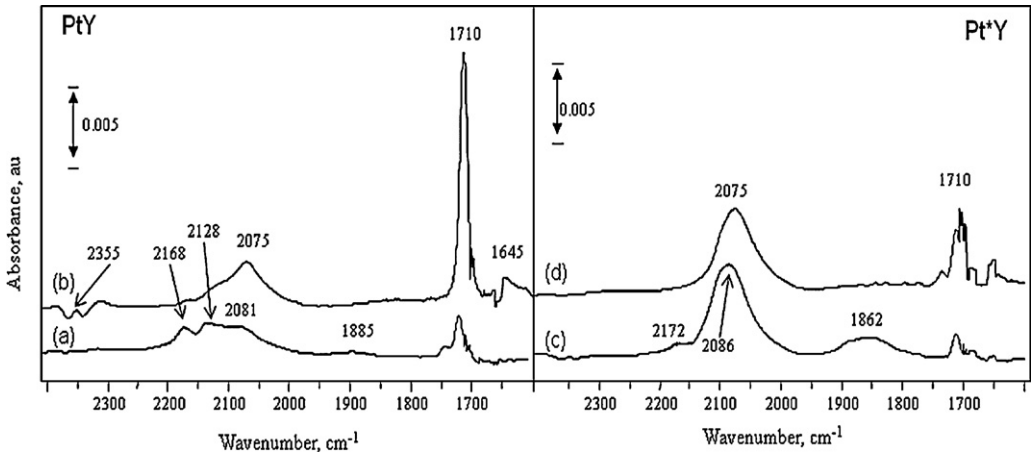

Fig. 5. FTIR spectra after admission of CO (10 Torr) over PtY and Pt*Y: (a and c) after 20 min of CO adsorption and (b and d) after evacation at RT.

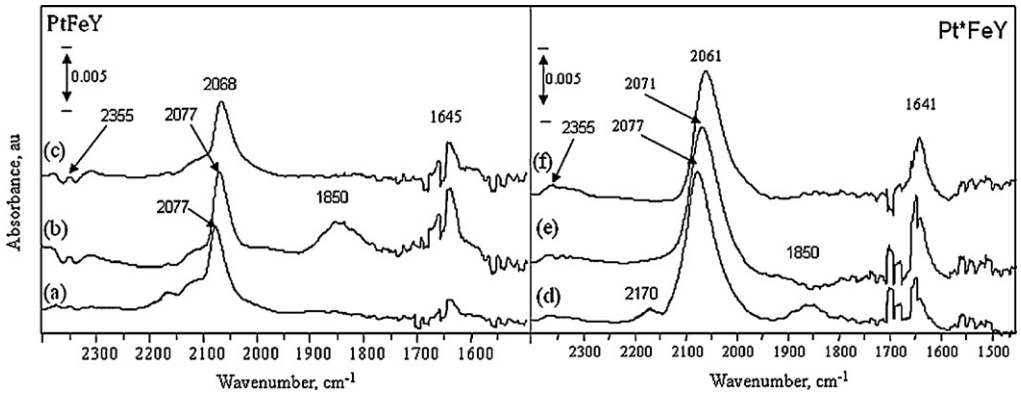

Fig. 6. FTIR spectra after admission of 10 Torr CO over PtFeY and Pt*FeY: (a and d) after 20 min of CO adsorption, (b and e) after evacation at RT, (c and f) after evacation at 50 °C.

intensity characteristic to carbonate species was observed in parallel with the disappearance of the peak at characteristic to CO adsorbed on cationic platinum and bridged $Pt^0{}_2CO$.

A comparison of Pt–CO bond position on Fe-free and Fe-promoted PtY after admission of CO gas at RT revealed a decrease in the absolute band frequency of Pt^0–CO with ≈4 and 9 cm^{-1} in as prepared and reduced samples, respectively. Such decrease of the absolute band frequency after Fe modifications may be due to a dipole–dipole coupling between neighboring adsorbed CO molecules [48,49]. Furthermore, Ishikawa et al. [50] reported that for most of the mixed Pt–M metal surfaces, the presence of M weakens the Pt–C bond and lowers the C–O stretching frequency. From forgoing, Pt particles may be partially covered with Fe atoms which leads to strong interaction of Fe and Pt in Fe–Pt and hence modifies the electronic states of Pt metal. As a result, Pt^0–CO bond becomes longer and Fe-oxide provides active oxygen for CO oxidation [11]. All of these parameters should modify the catalytic activity of the Fe-promoted PtY catalyst as will be mentioned later on.

3.2. The catalytic activity measurements of the prepared catalysts

3.2.1. CO oxidation by O_2 gas

Fig. 7 shows the temperature dependence of the reaction on the IR spectra measured due to CO oxidation by O_2 ($CO/O_2 = 1$) over PtY and Pt*Y catalysts. The exposure of PtY catalyst to $CO + O_2$ gas mixture at RT after 20 min of gas adsorption (Fig. 7a) presents only a small band attributed to linear Pt^0–CO at 2075 cm^{-1}. No peaks due to methanation of CO were observed under the conditions of the present study. With increasing the cell temperature to 50 °C and 100 °C, the spectra in Fig. 7b and c presented a peak characteristic for linear Pt^0–CO with small peak corresponds to carbonyl (–C=O) in carboxylate species around 1710 cm^{-1}. Additionally, small amounts of adsorbed CO_2 were also observed at 2355 cm^{-1} as well.

In case of Pt*Y sample, the spectrum taken at RT (Fig. 7d) shows three peaks at 2090, 1860 and 2355 cm^{-1} due to linear Pt^0–CO, bridged $Pt^0{}_2CO$ and adsorbed species of CO_2, respectively. After increasing the temperature of the cell to 50 °C and 100 °C, the intensity of CO_2 peak increased. Unexpectedly, the peaks characteristic to on top linear Pt^0–CO (at 2090 cm^{-1}) and bridged $Pt^0{}_2CO$ (at 1860 cm^{-1}) increased. The CO oxidation by O_2 over Pt*Y did not show any carbonate or carboxylate species, i.e. CO_2 was the only oxidation product of CO on the surface of Pt*Y.

It is widely accepted that CO oxidation on Pt metal follows a Langmuir–Hinshelwood single site mechanism [51,52] in which CO and O compete for the Pt sites. CO adsorbed on Pt reacts with O adsorbed on an adjacent Pt site. It was noticed that, carboxylate and carbonate species were observed after adsorption of CO as a single gas without the formation of considerable amount of CO_2. In this case there was no sufficient amount of oxygen present in the reaction medium. Moreover, carboxylate species were observed during CO oxidation by O_2 over unreduced catalyst (PtY) which has less number of metallic Pt sites. Furthermore, higher amount of CO_2 was formed during CO oxidation by O_2 over reduced sample (Pt*Y) where greater number of Pt sites are available. The previous observations indicate that carbonyl species (carboxylate and/or

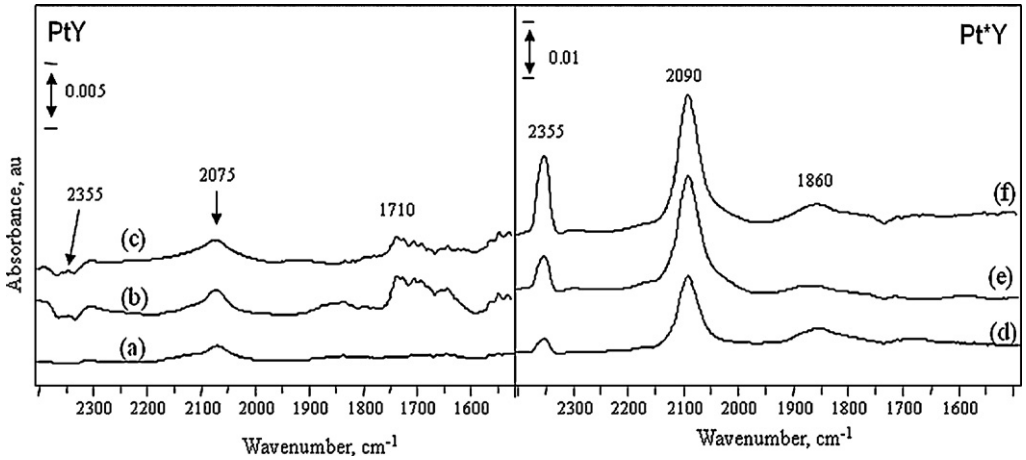

Fig. 7. In situ FTIR spectra of the $CO + O_2$ (10:10) gas mixture adsorbed on PtY and Pt*Y as a function of temperature; (a and d) RT, (b and e) heated at 50 °C and (c and f) heated at 100 °C.

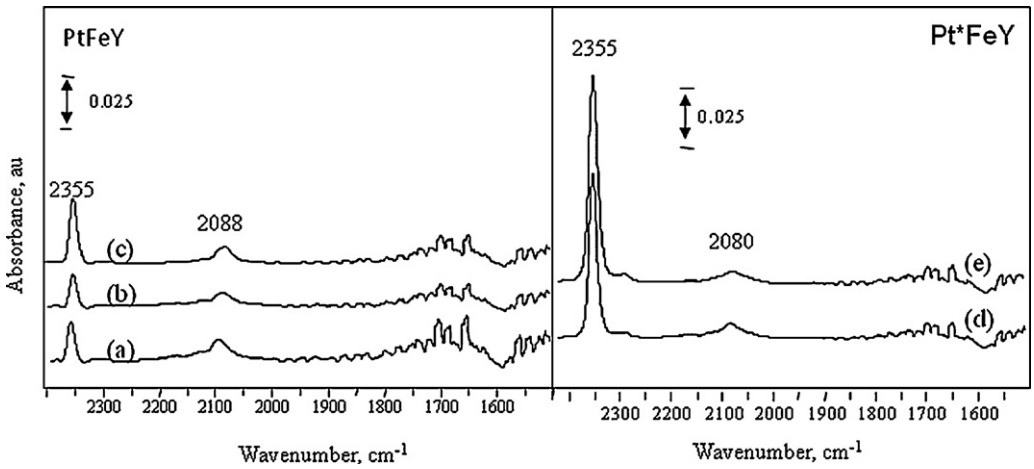

Fig. 8. In situ FTIR spectra of the CO + O_2 (10:10) gas mixture adsorbed on PtFeY and Pt*FeY as a function of temperature; (a and d) RT, (b and e) heated at 50 °C and (c) heated at 100 °C.

carbonate) may be considered as an intermediate to CO_2 formation on Pt sites in PtY catalyst since CO_2 is formed in the presence of sufficient amount of O_2 and vacant adsorption Pt sites, Eqs. (1)–(4).

$$CO + Pt \rightarrow OC{\cdot}Pt \quad (1)$$

$$O_2 + Pt \rightarrow 2O{\cdot}Pt \quad (2)$$

$$OC{\cdot}Pt + O{\cdot}Pt \rightarrow {}^{-}OOC{\cdot}Pt^{+}\,(\text{carboxylate}) + Pt \quad (3)$$

$${}^{-}OOC{\cdot}Pt^{+}\ \text{rearrangement}) \rightarrow CO_2{\cdot}Pt \quad (4)$$

To illustrate the promotion effect of Fe oxide on the catalytic activity of PtY towards CO oxidation by oxygen under the same previous conditions, CO + O_2 gas mixture was admitted over PtFeY catalyst and the spectra are presented in Fig. 8. Adsorption of the gas mixture on PtFeY at RT (Fig. 8a) produced a band at 2088 cm^{-1}, which is due to on top linear Pt^0–CO. The oxidation products of CO are resolved at 2355 cm^{-1} and 1650–1710 cm^{-1} due to adsorbed species of CO_2 and carbonyl species, respectively. Increasing the cell temperature to 50 °C and 100 °C (Fig. 8b and c) leads to an increase of adsorbed CO_2 peak at 2355 cm^{-1} but carboxylate and carbonate peaks did not change remarkably. It is clear that the amount of CO_2 formed over PtFeY is higher than the amount of CO_2 formed over both PtY and Pt*Y. These data are in agreement with TPD profiles in Fig. 4 since CO_2 was desorbed out of PtFeY surface at lower temperature than the desorption temperature out of PtY catalyst. This indicates the positive promotion effect of Fe on the catalytic activity of PtY which may be explained by the hypothesis that oxygen would have a greater probability for adsorption on PtFeY than the adsorption on PtY. Consequently, Fe oxide weakens the Pt–CO bond [50,53], provides more favorable sites for oxygen adsorption than Pt itself and locates in close contact with surface Pt [11,12,54].

For the reduced Fe oxide promoted PtY, the spectrum (Fig. 8d) taken at RT after 20 min of gas mixing shows small peaks characteristic to linear Pt^0–CO (at 2088 cm^{-1}) with a pronounced amount of adsorbed CO_2 detected at 2355 cm^{-1}. Increasing the cell temperature to 50 °C led to the increase of CO_2 characteristic peak (Fig. 8e). The amount of CO_2 detected on the reduced sample is much greater than the amount of CO_2 detected on the surface of unreduced sample. In addition, the amount of adsorbed CO detected in case of Pt*FeY is higher than that in case of PtFeY, Fig. 6. As previously reported Fe is present as Fe^{2+} and/or Fe^{3+} but not as Fe^0 according to the reduction conditions [11]. Hence, in addition to the Langmuir–Hinshelwood mechanism proposed for PtY, oxygen may be dissociatively adsorbed on Fe oxide with oxidation of the CO at the interface between Fe oxide and Pt or via the oxygen spillover to the Pt sites as discussed previously [2]. This creates a noncompetitive site for oxygen such that it no longer must compete with CO for the Pt sites [2].

3.2.2. Water-gas shift reaction

Fig. 9 shows the IR spectra in the region of 2400–1500 cm^{-1} obtained when PtY catalyst was exposed to the gas mixture of

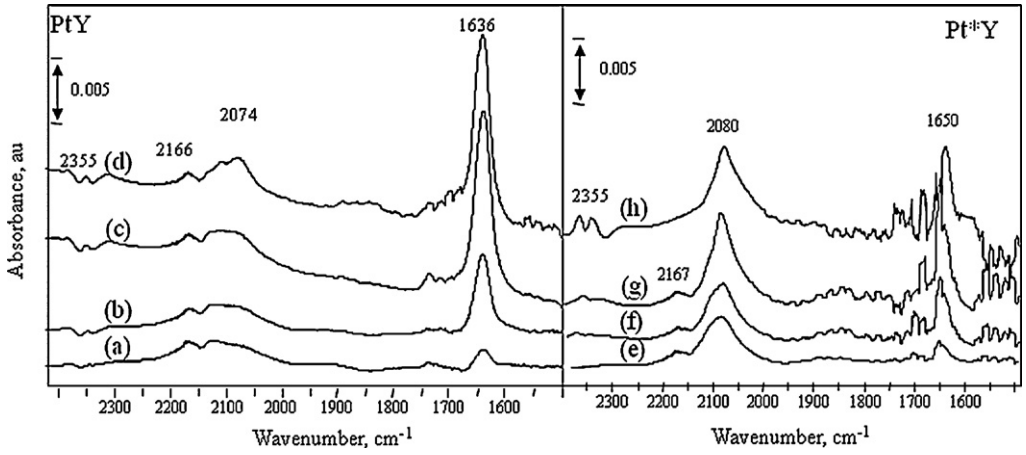

Fig. 9. In situ FTIR spectra of the CO + H_2O (15:1) gas mixture adsorbed on PtY and Pt*Y as a function of reaction time and temperature; (a and e) 0.5 min of gas adsorption at RT, (b and f) 20 min of gas adsorption at RT, (c and g) heated at 50 °C and (d and h) heated at 100 °C.

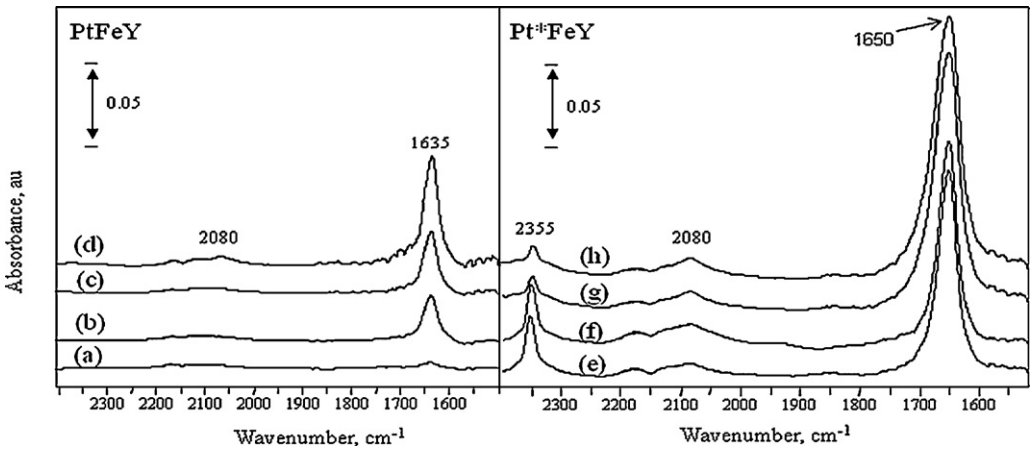

Fig. 10. In situ FTIR spectra of the CO + H_2O (15:1) gas mixture adsorbed on PtFeY and Pt*FeY as a function of reaction time and temperature; (a and e) one min of gas adsorption at RT, (b and f) 20 min of gas adsorption at RT, (c and g) heated at 50 °C and (d and h) heated at 100 °C.

CO + H_2O (15:1) at RT as a function of reaction temperature. The initial spectrum, recorded after 0.5 min of contact time (Fig. 9a) shows a small peak at 1636 cm^{-1} and weak peaks at 2074 and 2166 cm^{-1} characteristic to linear Pt^0–CO and CO adsorbed on Pt cationic species (Pt^{n+}CO), respectively. It is well known that the peak at 1636 cm^{-1} may be due to carbonate species or δ(H_2O) mode of adsorbed water, which lies in this region as well [55]. This peak was not shifted upon using D_2O instead of H_2O (not shown). The preservation of this band after isotope admission confirmed that it does not contain hydrogen atoms. Thus the band is assigned to carbonate species.

Increasing contact time to 20 min leads to the increase of linear Pt^0–CO (Fig. 9b). This may be due to the increase of Pt metal sites formed from the reduction of Pt^{n+} under the reaction conditions. Also the peak characteristic to carbonate species increased. With raising reaction temperature to 50 and 100 °C (Fig. 9c and d), the intensity of the peak characteristic to carbonate at 1636 cm^{-1} progressively increased and also a small peak related to adsorbed species of CO_2 at 2355 cm^{-1} was also observed.

The IR spectrum measured after 0.5 min of gas mixture adsorption (CO + H_2O) at RT onto Pt*Y (Fig. 9e) shows two peaks at 2080 and 2167 cm^{-1} due to Pt^0–CO and Pt^{n+}CO, respectively, besides a small peak at 1650 cm^{-1} related to carbonate species indicating the initiation of the reaction just after the addition of the gas mixture to the catalyst surface. The spectrum recorded after 20 min of contact time (Fig. 9f) presented an increase of the peak characteristic to carbonate species at 1650 cm^{-1}. Increasing the cell temperature to 50 °C and 100 °C (Fig. 9g and h) leads to an increase of the peak related to CO_3^{2-} and the appearance of trace amount of CO_2 that detected at 2355 cm^{-1}. A relative increase of the peaks characteristic to Pt^0–CO in both PtY and Pt*Y was observed which indicates further reduction of the Pt^{n+} sites. Reduction of such Pt^{n+} ions occurs most probably by H_2 gas that evolved from WGS reaction.

Fig. 10 shows the effect of reaction temperature on the changes undertaken on IR spectra after admission of gas mixture of CO + H_2O (15:1) over PtFeY and Pt*FeY catalysts. In case of the PtFeY, the spectrum taken after 1 min shows a very small peak characteristic to CO_3^{2-} at 1635 cm^{-1} indicating the initiation of the reaction as soon as admitting the gas mixture to the catalyst surface. After 20 min of contact time at RT and after elevation of the reaction temperature to 50 °C and 100 °C (Fig. 10b–d) the spectra show the growth of the carbonate peak without the appearance of any other peaks.

On the other hand, the spectrum recorded after 1 min of gas mixture admission (CO + H_2O) over Pt*FeY, Fig. 10e, displayed a strong peak at 1650 cm^{-1} due to carbonate and another peak at 2355 cm^{-1} related to the adsorbed CO_2. In addition, weak peaks at 2080 and 2170 cm^{-1} due to Pt^0–CO and Pt^{n+}CO were observed. After 20 min of reaction time and increasing the reaction temperature to 50° and 100 °C, Fig. 10f–h, the intensity of CO_2 peak decreased with a parallel increase of the peak characteristic for carbonate species. This confirms the proposition that CO_2 is an intermediate for CO_3^{2-} in WGSR over Pt*FeY whereas in case of PtY catalyst, the carbonyl is considered to be an intermediate for CO_2. Comparing the spectra taken after adsorption of gases over PtFeY and over Pt*FeY, it may be concluded that the catalytic activity towards the formation of car-

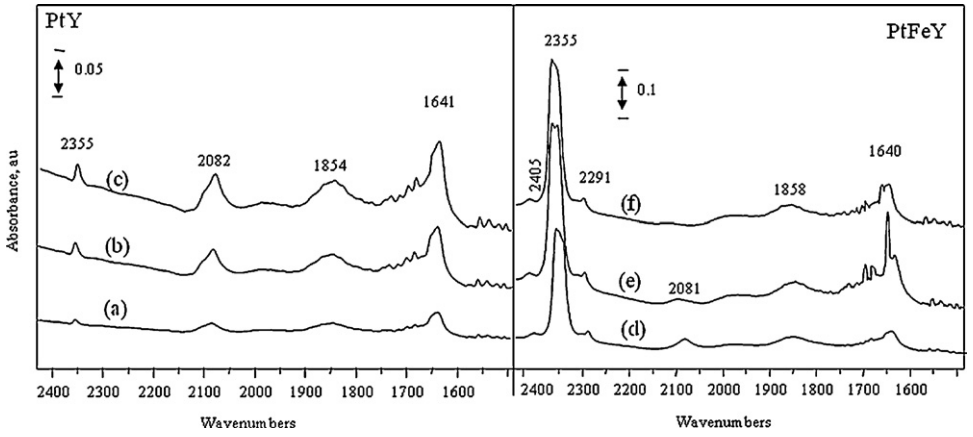

Fig. 11. In situ FTIR spectra of CO + O_2 + H_2O (15:15:1) adsorbed over PtY and PtFeY: (a and d) after 20 min at RT (b and e) heated at 50 °C and (c and f) heated at 100 °C.

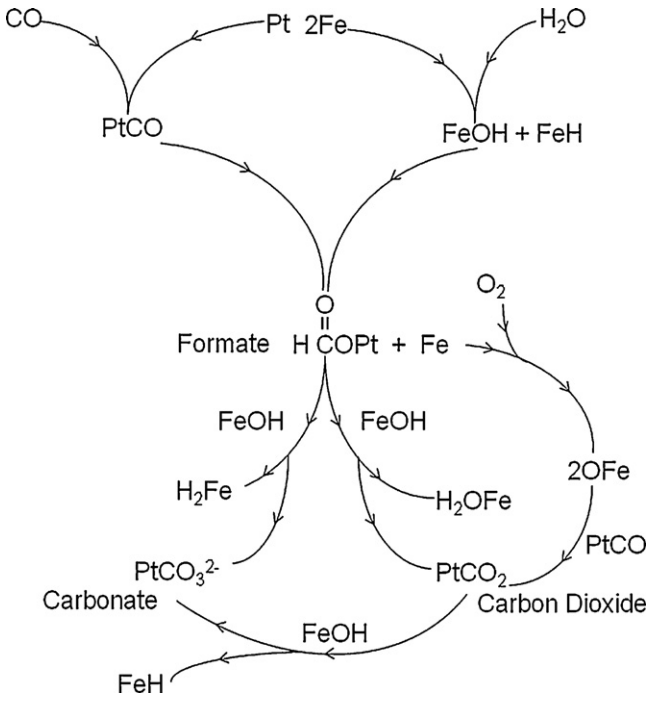

Scheme 1. Proposed scheme of CO oxidation over the employed catalysts.

bonate species in WGSR is higher for the reduced sample than that of the as prepared one. Additionally, by inspection of the IR spectra recorded after admission of $CO + H_2O$ gas mixture to PtY and PtFeY, it is noticed that the amount of carbonate species detected over PtFeY (as a function of the peak intensity) is greatly higher than that detected over Fe-free PtY samples. This reflects that, in presence of H_2O, Fe has a positive effect towards the oxidation of CO to carbonate species.

Moreover, the mechanism of WGSR may change in presence of Fe oxide beside Pt metal atoms. It was reported that the addition of water vapor improves the oxidation of CO over PtFe containing catalysts due to the difference in the oxidative states of the metals present on the surface. According to Langmuir–Hinshelwood mechanism CO competitively adsorbed on Pt with O_2 and the strength of adsorbed CO decreases with decreasing Pt oxidation state [8,56,57]. However the reaction may work via dual site mechanism rather than Langmuir–Hinshelwood single site mechanism in presence of Fe oxide. It has been shown from the results that H_2O improves CO oxidation over Pt containing catalysts more than the oxidative state of Pt itself or molecular oxygen. This may be due to the increase of the activity in presence of hydroxyl group [58,59].

It is clear in this work that, addition of Fe to PtY catalyst greatly enhances the catalytic activity towards CO oxidation. The superior activity of PtFeY in presence of water vapor may result from the increase of the number of weak and medium basic sites after promotion with Fe oxide as presented in the TPD data after CO and $CO + O_2$ adsorption. The concentration of hydroxyl groups increased with increasing basicity of the catalyst surface under humid conditions [35]. In addition, Fe oxide provides adsorption sites for oxygen and/or OH group whereas Pt sites provide adsorption sites for CO. For WGSR, it was reported that CO reacts with the OH groups on the surface to generate formate species adsorbed on the catalyst surface. This is supported by the detection of small amounts of formate and formic acid species in TPD experiment. The formates are then decomposed in presence of Fe–OH to give CO_2 and H_2 [60,61] or carbonate species [62], which is detected in this work and can be proposed in Scheme 1. These may strengthen the proposition that the reaction follows a noncompetitive duel-site mechanism in

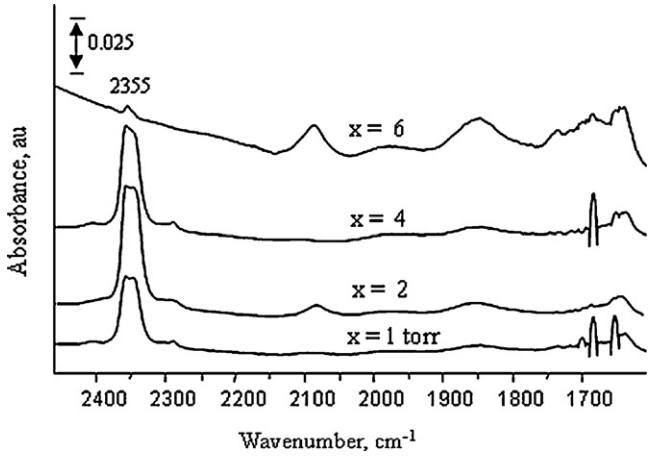

Fig. 12. In situ FTIR spectra of $CO + O_2 + H_2O$ (15:15:*x*) (*x* = 1, 2, 4, 6 Torr) adsorbed over PtFeY catalyst after heating at 50 °C.

the oxidation of CO in presence of PtFe system. This is in consistent with a previous report by Kotobuki et al. [10].

3.2.3. Effect of water on the oxidation of CO

The in situ FTIR spectra in the range of 2400–1500 cm^{-1} under the reaction conditions were measured after admission of gas mixture ($CO:O_2:H_2O$; 10:10:1) at RT over PtY and PtFeY and the spectra are shown in Fig. 11. Inspection of the spectra recorded after admission of gas mixture at RT, Fig. 11a, reveals that small peaks due to Pt^0–CO and $Pt^0{}_2CO$ were observed at 2082 and 1854 cm^{-1}, respectively. Two types of CO oxidation products were detected namely, adsorbed CO_2 at 2355 cm^{-1} and carbonate species at 1641 cm^{-1}. With increasing the cell temperature to 50 and 100 °C, Fig. 11b and c, slight increase in the intensity of the peaks characteristic to CO_2 and carbonate species was observed. The slight increase of the oxidation products of CO may be attributed to the decrease of the strength of CO adsorption which leads to CO desorption out of the surface and leaves vacant sites for O_2 and H_2O. Therefore CO oxidation is accomplished according to Langmuir–Hinshelwood mechanism.

Fig. 11d shows the spectrum taken after 20 min of admission of the gas mixture ($CO + O_2 + H_2O$; 10:10:1) over PtFeY to shed light on the effect of introducing water vapor during CO oxidation by O_2 (more realistic conditions). The spectrum showed small peaks at 2081 and 1858 cm^{-1} due to Pt^0–CO and $Pt^0{}_2CO$, respectively. A strong peak at 2355 cm^{-1} was observed with small peaks at 2405 and 2291 cm^{-1}. These peaks are due to adsorbed species of CO_2 on different sites [46]. The presence of such peaks indicates the high activity of Fe oxide promoted PtY catalyst. In addition, small amount of carbonate species was formed and detected at 1640 cm^{-1}. With increasing reaction temperature (Fig. 11e and f), an increase of the intensity of the peak related to carbonate species (at 1640 cm^{-1}) and adsorbed species of CO_2 was observed. The appearance of CO_2 as high intensity double peak at 2356 and 2348 cm^{-1} and small peaks at 2405 and 2291 cm^{-1} indicates that the Fe-containing PtY catalyst has heterogeneous nature with different adsorption sites for CO_2. Also, PtY is strongly active towards the formation of CO_2 after modification with Fe.

The effect of the amount of water vapor in the admitted gas mixture on the catalytic activity was carried out by changing the gas mixture ratio ($CO + O_2 + H_2O$) (15:15:*x*; *x* = 1, 2, 4, 6 Torr) on PtFeY. The measured spectra are presented in Fig. 12. The intensity of CO_2 peak increased after increasing the amount of water to 2 Torr. Further increase of water addition led to a decrease in the CO_2 intensity. It may be suggested that the activity decreases increase with the amount of added water is due the competition of

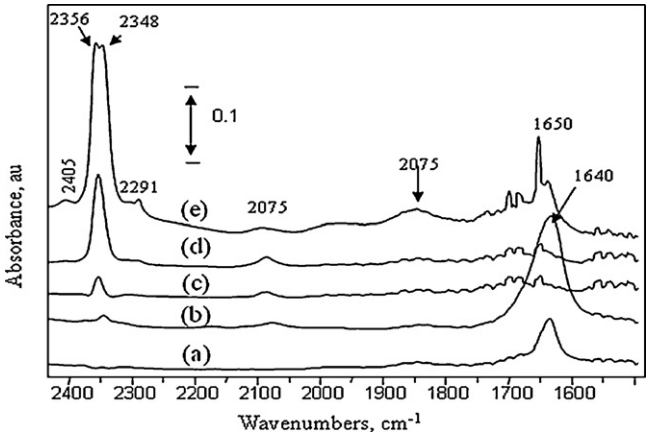

Fig. 13. Comparison between the spectra obtained after admission of different gas mixtures over as prepared and reduced PtFeY: (a) $CO + H_2O$)/PtFeY, (b) $(CO + H_2O)$/Pt*FeY, (c) $(CO + O_2)$/PtFeY, (d) $(CO + O_2)$/Pt*FeY and (e) $(H_2O + O_2 + CO)$/PtFeY.

gases in the adsorption to the surface of the catalyst (i.e. competitive adsorption) [63–67].

The activity of PtFeY catalyst was improved with reactants containing trace amount of water. Fig. 13 shows a comparison between the spectra taken for CO removal reactions at 50 °C for PtFeY and Pt*FeY using different reaction gas mixtures. The tendency to form CO_2 is high after admission of $CO + O_2$ gas mixture over the employed catalyst. However the tendency to form carbonate species is high after admission of $CO + H_2O$ gas mixture over the PtFeY catalyst. The oxidation of CO by O_2 in presence of trace amount of water ($CO + O_2 + H_2O$) leads to a pronounced enhancement in the catalytic activity towards the formation of CO_2 since an abrubt increase of the amount of CO_2 detected in the IR spectra, Fig. 13e. Considering that the area under peak reflects the concentration of CO_2 adsorbed on the surface, the former was measured and listed in Table 2 to roughly compare between the amount of CO_2 produced over PtY and Fe-promoted PtY catalysts after using O_2 to oxidize CO in presence or absence of H_2O. It is apparent that, the addition of H_2O to the gas mixture over PtY increased the area under peak around 70 times more than that of PtY without water. However the addition of water to PtFeY increased the area under peak around 5 times more than that in case of PtFeY without water. We should note also that the area under CO_2 peak over PtFeY is more than 100 times greater than that over PtY. In general, the oxidation of CO with O_2 gas leads to the increase of CO_2 formation in the order of PtY < Pt*Y < PtY(H_2O) < PtFeY < Pt*FeY < PtFeY(H_2O); where (H_2O) denotes to the addition of 1 Torr of water vapor to the gas mixture. The area under CO_2 peak in case of PtFeY(H_2O) is almost 600 times more than the area under CO_2 peak in case of Fe-free PtY catalyst. A number of explanations have been proposed for the enhancement of activity in the presence of H_2O. One was that water enhances the water gas shift reaction and as a result more CO was converted into CO_2. The second possibility was that the hydroxyl group formed on the catalyst upon adsorption of water was a better oxidant than oxygen itself and consequently increases the oxidation of CO [6,21] and produces CO_2, Scheme 1. Finally, the presence of water leads to the formation of hydroxyl groups on the catalyst surface which leads to the decrease of CO–Pt strength [20] and it will have the chance to produce either CO_2 or carbonate species as demonstrated in Scheme 1.

Table 2
Absorbance and relative area under peak of CO oxidation in presence and absence of water over Fe-free and Fe-promoted PtY catalysts.

Catalyst	Gas mixture	Abs. (au)	Relative area under peak
PtY	$O_2 + CO$	0.018	1
Pt*Y	$O_2 + CO$	0.65	51
PtY	$O_2 + CO + H_2O$	0.48	70
PtFeY	$O_2 + CO$	1.94	117
Pt*FeY	$O_2 + CO$	15.2	142
PtFeY	$O_2 + CO + H_2O$	32.2	605

4. Conclusions

Promotion of PtY with Fe-oxide has great impact on the morphology of the catalyst surface as well as on the catalytic activity. The effect of Fe-promotion will be summarized as follows:

1. The Pt particles were dispersed homogeneously on the catalyst surface.
2. Pt particle size decreased with Fe promotion from ≈18–20 nm in case of PtY to 8–15 nm in case Fe-promoted PtY catalyst.
3. The presence of Fe-oxide besides Pt particles caused the presence of low temperature CO-TPD desorption peak. This peak indicates the presence of OH group on the Pt–Fe surface.
4. Fe-oxide increased the accessible adsorption sites for the O_2 gas or H_2O vapor. This leads to the increase of the catalytic activity even at low temperature.
5. The activity towards the formation of CO_2 was generally in the order of Pt*FeY > PtFeY > Pt*Y > PtY which means that it is higher in presence of Fe-oxide as a promoter and after reduction.

Besides the promotion effect with Fe addition, a great enhancement effect on the catalytic activity of CO oxidation over the surface of PtFeY catalyst was noticed with addition of trace amount of water. The amount of CO_2 adsorbed over PtFeY increased around 5 and 600 times more than the activity without water over PtFeY and Fe-free PtY catalysts, respectively.

References

[1] S. Guerrero, J.T. Miller, A.J. Kropf, E.E. Wolf, J. Catal. 262 (2009) 102–110.
[2] S.K. Jain, E.M. Crabb, L.E. Smart, D. Thompsett, A.M. Steele, Appl. Catal. B 89 (2009) 349–355.
[3] S.D. Gardner, G.B. Hound, B.T. Upchurch, D.R. Schryer, E.J. Kielin, J. Schryer, J. Catal. 129 (1991) 114–120.
[4] M. Haruta, N. Yamada, T. Kobayashi, S. Iijima, J. Catal. 115 (1989) 301–309.
[5] D.R. Schryer, B.T. Upchurch, J.D. Van Norman, K.G. Brown, J. Schryer, J. Catal. 122 (1990) 193–197.
[6] A. Manasilp, E. Gulari, Appl. Catal. B 37 (2002) 17–25.
[7] S.H. Oh, R.M. Sinkevitch, J. Catal. 142 (1993) 254–262.
[8] A. Sirijaruphan, J.G. Goodwin Jr., R.W. Rice, J. Catal. 221 (2004) 288–293.
[9] K. Arnby, M. Rahmani, M. Sanati, N. Cruise, A. Amberntsson, M. Skoglundh, Appl. Catal. B 54 (2004) 1–7.
[10] M. Kotobuki, A. Watanabe, H. Uchida, H. Yamashita, M. Watanabe, J. Catal. 236 (2005) 262–269.
[11] X. Liu, O. Korotkikh, R. Farrauto, Appl. Catal. A 226 (2002) 293–303.
[12] A. Sirijaruphan, J.G. Goodwin Jr., R.W. Rice, J. Catal. 224 (2004) 304–313.
[13] I. Rosso, C. Galletti, G. Saracco, E. Garrone, V. Specchia, Appl. Catal. B 48 (2004) 195–203.
[14] Y. Hasegawa, K.I. Sotowa, K. Kusakabe, S. Morooka, Micro. Meso. Mater. 53 (2002) 37–43.
[15] T.M. Salama, Z.M. El-Bahy, F.I. Zidan, J. Mol. Catal. A 264 (2007) 128–134.
[16] H. Pan, M. Xu, Z. Li, S. Huang, C. He, Chemosphere 76 (2009) 721–726.
[17] M.A. Debeila, R.P.K. Wells, J.A. Anderson, J. Catal. 239 (2006) 162–172.
[18] H. Ohtsuka, T. Tabata, Appl. Catal. B 21 (1999) 133–139.
[19] S. Monyanon, S. Pongstabodee, A. Luengnaruemitchai, J. Power Sources 163 (2006) 547–554.
[20] H.J. Kwon, J.H. Baik, Y.T. Kwon, I.S. Nam, S.H. Oh, Chem. Eng. J. 141 (2008) 194–203.
[21] A. Parinyaswan, S. Pongstabodee, A. Luengnaruemitchai, Int. J. Hydrogen Energy 31 (2006) 1942–1949.
[22] S.D. Ebbesen, B.L. Mojet, L. Lefferts, J. Catal 246 (2007) 66–73.
[23] P. Klug, L.E. Alexander, Direction Procedures for Polycrystalline and Amorphous Materials, Wiley, 1954.
[24] B. Atalik, D. Uner, J. Catal. 241 (2006) 268–275.
[25] W.H. Quayle, G. Peeters, G.L. De Roy, E.F. Vansant, J.H. Lunsford, Inorg. Chem. 21 (1982) 2226–2231.

[26] A. Tömcrona, M. Skoglundh, P. Thormiihlen, E. Fridell, E. Jobson, Appl. Catal. B 14 (1997) 131–146.
[27] J. Scherzer, J.L. Bass, J. Catal. 28 (1973) 101–115.
[28] R. Cid, F.J. Gil Lambfas, J.L.G. Fierro, A. Lopez Agudo, J. Villasenor, J. Catal. 89 (1984) 478–488.
[29] Y. Zang, R. Farnood, Appl. Catal. B 79 (2008) 334–340.
[30] V. Matolin, I. Matolinov, F. Sutara, K. Veltrusk, Surf. Sci. 566–568 (2004) 1093–1096.
[31] P. Thormählen, M. Skoglundh, E. Fridell, B. Andersson, J. Catal. 188 (1999) 300–310.
[32] R. Padilla, M. Benito, L. Rodríguez, A.S. Lotina, L. Daza, J. Power Sources 192 (2009) 114–119.
[33] D.R. Mullins, K.Z. Zhang, Surf. Sci. 513 (2002) 163–173.
[34] Z. Jiang, W. Huang, H. Zhao, Z. Zhang, D. Tan, X. Bao, J. Mol. Catal. A 268 (2007) 213–220.
[35] S.H. Cho, J.S. Park, S.H. Choi, S.H. Kim, J. Power Sources 156 (2006) 260–266.
[36] K.I. Hadjiivanov, G.N. Vayssilov, Adv. Catal. 47 (2002) 307–511.
[37] P. Hollins, Surf. Sci. Rep. 16 (1992) 51–94.
[38] T. Rades, V.Y. Borovkov, V.B. Kazansky, M. Polisset-Thfoin, J. Fraissard, J. Phys. Chem. 100 (1996) 16238–16241.
[39] K. Chakarova, M. Mihaylov, K. Hadjiivaniov, Micro. Meso. Mater. 81 (2005) 305–312.
[40] K. Chakarova, M. Mihaylov, K. Hadjiivaniov, Catal. Comm. 6 (2005) 466–471.
[41] K. Chakarova, K. Hadjiivanov, G. Atanasova, K. Tenchev, J. Mol. Catal. A 264 (2007) 270–279.
[42] S. Albertazzi, G. Busca, E. Finocchio, R. Glőckler, A. Vaccari, J. Catal. 223 (2004) 372–381.
[43] S.T. Hong, M. Matsuoka, M. Anpo, Catal. Lett. 107 (2006) 173–176.
[44] K. Kinoshita, Carbon, Electrochemical and Physical Properties, Wiley, New York, 1988.
[45] T.M. Salama, R. Ohnishi, M. Ichikawa, J. Chem. Soc. Faraday Trans. 92 (1996) 301–306.
[46] M.M. Mohamed, M. Ichikawa, J. Colloid Interface Sci. 232 (2000) 381–388.
[47] T. Tanabe, R. Buckmaster, T. Ishibashi, T. Wadayama, A. Hatta, Surf. Sci. 472 (2001) 1–8.
[48] S. Tillmann, G. Samjeské, K.A. Friedrich, H. Baltruschat, Electrochim. Acta 49 (2003) 73–83.
[49] Z. Gandao, B. Coq, L. Charles de Mnorval, D. Tichit, Appl. Catal. A 147 (1996) 395–406.
[50] Y. Ishikawa, M. Liao, C.R. Cabrera, Surf. Sci. 513 (2002) 98–110.
[51] G. Ertl, Surf. Sci. 299 (1994) 742–754.
[52] J. Wintterlin, S. Völkening, J.V.W. Janssens, G. Ertl, Science 278 (1997) 1931–1934.
[53] M. Watanabe, H. Uchida, K. Ohkubo, H. Igarashi, Appl. Catal. B 46 (2003) 595–600.
[54] O. Korotkikh, R. Farrauto, Catal. Today 62 (2000) 249–254.
[55] M. Ahrens, O. Marie, P. Bazin, M. Daturi, J. Catal. 271 (2010) 1–11.
[56] A. Wootsch, C. Descorme, D. Duprez, J. Catal. 225 (2004) 259–266.
[57] G. Jacobs, U.M. Graham, E. Chenu, P.M. Patterson, A. Dozier, B.H. Davis, J. Catal. 229 (2005) 499–512.
[58] M.J. Kahlich, H.A. Gasteiger, R.J. Behm, J. Catal. 171 (1997) 93–105.
[59] H. Muraki, S.I. Matunaga, H. Shinjoh, M.S. Wainwright, D.L. Trimm, J. Chem. Tech. Biotechnol. 52 (1991) 415–424.
[60] T. Shido, Y. Iwasawa, J. Catal. 141 (1993) 71–81.
[61] G. Jacobs, A. Crawford, L. Williams, P.M. Patterson, B.H. Davis, Appl. Catal. A 267 (2004) 27–33.
[62] D. Teschner, A. Wootsch, O. Pozdnyakova-Tellinger, J. Kröhnert, E.M. Vass, M. Hävecker, S. Zafeiratos, P. Schnörch, P.C. Jentoft, A. Knop-Gericke, R. Schlögl, J. Catal. 249 (2007) 318–327.
[63] Z.M. ElBahy, R. Ohnishi, M. Ichikawa, Appl. Catal. B 40 (2003) 81–91.
[64] M. Jo, G. Kwon, W. Li, A.M. lane, J. Ind. Eng. Chem. 15 (2009) 336–341.
[65] G. Avgouropoulos, T. Ioannides, Appl. Catal. A 6424 (2003) 1–13.
[66] J. Jansson, A.E.C. Palmqvist, E. Fridell, M. Skoglundh, L. Osterlund, P. Thorahlen, V. Langer, J. Catal. 211 (2002) 387–397.
[67] Q.W. Chen, D.W. Bahnemann, J. Am. Chem. Soc. 122 (2000) 970–971.